Magnetostatic Wave Propagation in a Yttrium Iron Garnet (YIG)-Loaded Waveguide*

M. Radmanesh,
C.M. Chu
and
G.I. Haddad
Solid-State Electronics Laboratory
Department of Electrical and Computer Engineering
The University of Michigan
Ann Arbor, MI

The propagation of magnetostatic waves in a waveguide partially loaded with a YIG slab is investigated theoretically. The DC magnetic field is assumed to be parallel to the YIG slab and perpendicular to the direction of propagation. A dispersion relation is derived and sample numerical calculations of the propagation constant and the delay characteristics of the device are presented. It is found that the delay time per unit length can be controlled by the slab position in the waveguide and, furthermore, that the frequency range of operation of the device can be adjusted by the external magnetic bias field. The general formulation presented in this paper contains all the information given by the degenerate cases previously published. The special cases of interest are obtained simply as special cases of this general formulation.

Introduction

The purpose of this work was to study magnetostatic wave propagation in a rectangular waveguide partially filled with a low loss ferrite material. The dispersion relation and group time delay characteristics of the waves were investigated.

Magnetostatic waves are slow dispersive, magnetically dominated spin waves that propagate in magnetically biased ferrite slabs at microwave frequencies. The most common low loss ferrite material used for MSW propagation is epitaxial yttrium iron garnet (YIG).

The recent interest in MSW devices at microwave frequencies has accelerated because the growth of uniform, high quality, low loss epitaxial YIG films with a large aspect ratio has been improved and the design and fabrication of efficient RF to MSW transducers have been developed and realized.[1] The first development provides a uniform internal DC magnetic bias field so that many inhomogeneous transmission problems associated with non-uniform internal fields are eliminated.

The second development reduces coupling losses from RF waves to magnetostatic waves so that the overall insertion loss can be reduced greatly. Another motivation for exploring the use of magnetostatic waves in microwave signal processing is due to the fact that MSW operation is possible in the frequency range of 1.0 to 20.0 GHz with wide instantaneous bandwidths in contrast to surface acoustic wave (SAW) devices, which usually operate on the IF signal.

A comparison of the relative merits of MSW and SAW devices is given by Owens et al[2] and Collins et al[3] and is presented in Table 1. From this table it can be seen that the tunable properties, the lower propagation losses at microwave frequencies, the invariant transducer geometry, and the adjustable delay properties of magnetostatic wave devices present a major advantage in terms of device performance over SAW devices.

Based on recent literature,[4-9] the possible applications of MSW devices are summarized in Table 2. From this table, it can be seen that MSW devices cover a wide range of applications in microwave communication systems.

As noted in this table, their prime applications are in the areas of delay lines, filters, oscillators and resonators. The conventional means of exciting magnetostatic waves are by metal transducers that have been analyzed extensively in the literature.[10]

*This work was supported by the Air Force Systems Command, Avionics Laboratory, Wright-Patterson Air Force Base, Ohio under Contract No. F33615-81-K-1429.

TABLE I

CHARACTERISTIC FEATURES OF MSW AND SAW DEVICES[2,3]

Property	MSW	SAW
Maximum delay per cm	Hundreds of nS	Hundreds of μS
Transducer geometry	Simple/moderately complex	Complex
Transducer dimensions	Invariant with frequency	Decrease as frequency increases
Bandpass filtering capability	Good	Excellent
Adjustable delay	Yes	Not in a single device
Power handling	1 mW	1 W
Typical velocity (km/S)	10 to 1000	2 to 6
Typical attenuation (dB/μs)	5 at 1 GHz; 20 at 10 GHz	1 at 1 GHz; 60 at 10 GHz
Dispersion	Yes	No

TABLE II

PRIME APPLICATIONS OF MSW DEVICES

Device	Microwave Function
Non-dispersive delay line	Phase locking of pulsed oscillator, signal correlation, communication path length equalizer, rate sensor
Dispersive delay line	Group delay equalizer, pulse compression, compressive receiver, rate sensor, frequency synthesis
Tapped delay line	ECM deception, PSK matched filter, Fourier transformation
Variable delay line	Target simulation, electronic timing
Bandpass filter	ECM, radar, communication satellite repeaters
Tunable resonator	Narrowband frequency filter and oscillator applications
MSW directional coupler	Signal routing, switched delay line
MSW oscillator	Stable microwave source

Previous Investigations

Previous analyses of various types of geometries for MSW propagation have included the following:

- The first structure consisted of a YIG film deposited on a substrate and was investigated by Damon and Eshback.[11] The input and output transducers were microstrip lines. They determined the different propagating modes that can exist in this structure. A summary of all the propagating modes for different magnetization directions was reported by Adams et al[9]
- A multi-layer planar structure with ground planes was considered by Tsai et al[12] and others.[13] In this work, wave propagation in a normally magnetized structure of infinite width was analyzed. Daniel et al[14] reported a complete summary of the wave propagation in this structure for principal directions of magnetization
- Young[15] considered wave propagation in a metallic trough partially filled with YIG material. He derived the dispersion relation for two important propagating modes that can exist when magnetization is parallel to the slab plane
- Finally, a long rectangular YIG rod with metal boundaries was investigated by Auld and Mehta.[16] They studied two possible modes of propagation in this structure, using a mode analysis technique, and derived a dispersion relation for each case.

Using the developed formulation presented in this paper, the dispersion relations for three of the above cases (all but the third) are derived and the results are summarized in the section on degenerate cases.

Note that in all the reported structures, the YIG slab is inside an unbounded space except when the guide is completely filled. The case of a YIG slab enclosed in a waveguide, as shown in Figure 1, has never been studied.

This study concentrates on the theoretical analysis of magnetostatic wave propagation in a YIG slab inside a rectangular waveguide. The DC magnetic field is parallel to the slab and perpendicular to the direction of propagation. The slab is placed inside and along the guide, and to simplify analysis, the slab is assumed to be thin. The introduction of gap length (x_0) is motivated to account for the loose contract between the YIG slab and waveguide walls and to provide a general structure for the design of delay lines. In this paper, however, the case $x_0 = 0$ is treated in depth using the standard mode analysis technique, and the general case $x_0 \neq 0$ is left to further investigation.

Although no experiment was performed in this work, the computed results obtained by proper simulation were certainly in good agreement with the previous work.

An analytical expression for the dispersion relation is derived below. Numerical computation of the propagation constant and time delay per unit length in a certain frequency range and for particular values of DC magnetic field are presented in the section titled Numerical Results. In the section Degenerate Cases, some geometries that were treated previously are considered, and it is shown that these can be treated as special cases of the general formulation presented here.

Mode Analysis

As noted above, for the special case when $x_0 = 0$, the standard mode analysis technique is effective in finding the dispersion relations for magnetostatic wave propagation. The relative permeability tensor when $\underline{H}_{dc} = H_0\hat{x}$ can be expressed as follows:

$$\overline{T} = \begin{bmatrix} 1 & 0 & 0 \\ 0 & \mu & jK_1 \\ 0 & -jK_1 & \mu \end{bmatrix} \qquad (1)$$

where

$$\mu = 1 + \frac{\omega_0\omega_M}{\omega_0^2 - \omega^2}$$

$$K_1 = \frac{\omega\omega_M}{\omega_0^2 - \omega^2}$$

$\omega_0 = \mu_0\gamma H_0$ and

$\omega_M = \mu_0\gamma M_0$;

p2

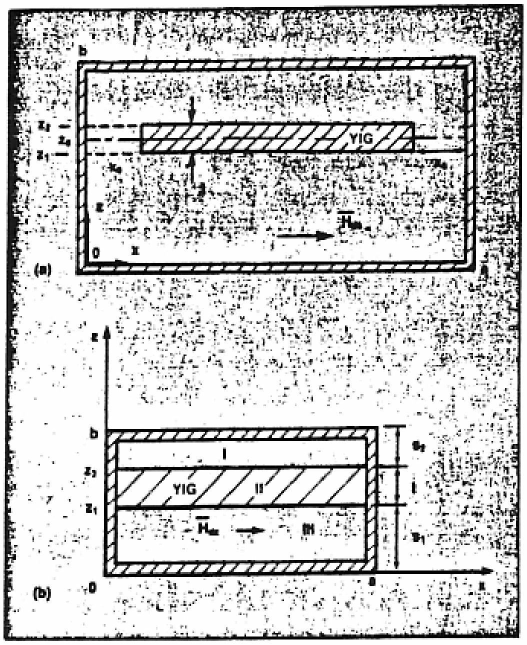

Fig. 1 Device geometry: (a) general case ($x_0 \neq 0$); (b) special case ($x_0 = 0$).

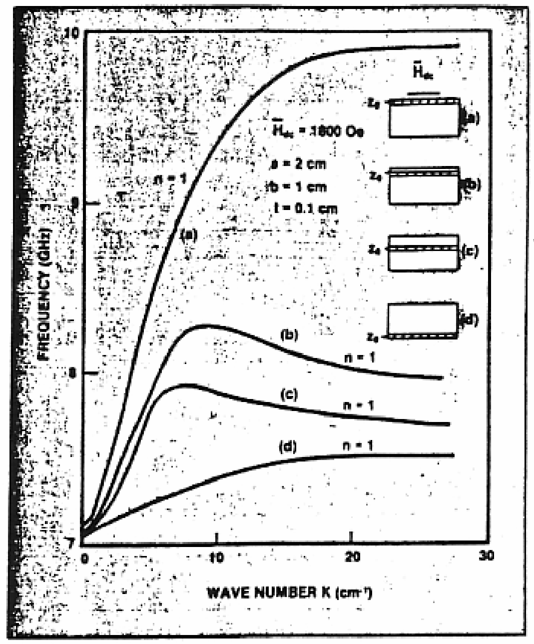

Fig. 2 Effect of slab position on the dispersion characteristics: (a) z_0 = 0.95 cm; (b) z_0 = 0.8 cm; (c) z_0 = 0.7 cm; and (d) z_0 = 0.05 cm.

μ_0 and γ are the free space permeability constant and gyromagnetic constant, respectively; ω is the operating frequency; and H_0 and M_0 are the internal magnetic field and saturation magnetization, respectively.[17]

Note that the internal magnetic field (H_0) is given by[18] $H_0 = H_{dc} - N_x M_0$ where N_x is the demagnetizing factor in the x-direction. For a thin slab with the z-axis perpendicular to the broad face, $N_x = 0$. Therefore, in this analysis to the first order of approximation, the demagnetizing fields are neglected and $H_0 = H_{dc}$.

For magnetostatic waves, the magnetic field H is given by

$$\bar{H} = \nabla \phi \qquad (2)$$

where ϕ is the scalar magnetic potential satisfying

$$\phi_{xx} + \phi_{yy} + \phi_{zz} = 0 \qquad (3)$$

in the air region (Regions I and III in Figure 1) and

$$\phi_{xx} + \mu\,(\phi_{yy} + \phi_{zz}) = 0 \qquad (4)$$

in the YIG region (Region II). The boundary conditions to be satisfied are:

1. $B_x = 0$ at $x = 0$ and a.
2. $B_z = 0$ at $z = 0$ and b.
3. ϕ is continuous at the interfaces $z = z_1$ and z_2.
4. B_z is continuous at the interfaces $z = z_1$ and z_2.

The implied time dependence is $e^{j\omega t}$ and is omitted in the expressions. The variation of ϕ in the axial direction is assumed to be of the form e^{-jky}. The following forms of ϕ in the three regions satisfy boundary conditions 1 and 2 and can be expressed as

$$\phi_1 = \sum_{n=0}^{\infty} A_n \cos\frac{n\pi}{a}x \cosh \gamma_n'(b - z)\, e^{-jky}, \qquad (5)$$

$$\phi_2 = \sum_{n=0}^{\infty} \cos\frac{n\pi}{a}x\,(B_n \cosh \gamma_n z + C_n \sinh \gamma_n z)\, e^{-jky} \qquad (6)$$

and

$$\phi_3 = \sum_{n=0}^{\infty} D_n \cos\frac{n\pi}{a}x \cosh \gamma_n' z\, e^{-jky} \qquad (7)$$

where A_n, B_n, C_n and D_n are constants and γ'_n and γ_n are phase constants given by

$$\gamma_n' = \left[K^2 + \left(\frac{n\pi}{a}\right)^2\right]^{1/2} \qquad (8)$$

and

$$\gamma_n = \left[K^2 + \frac{1}{\mu}\left(\frac{n\pi}{a}\right)^2\right]^{1/2} \qquad (9)$$

where n = 1,2,3.... For each n(each mode), applying the boundary conditions 2 and 4 yields the linear equations in A_n, B_n, C_n and D_n that can be found at the bottom of page 138.

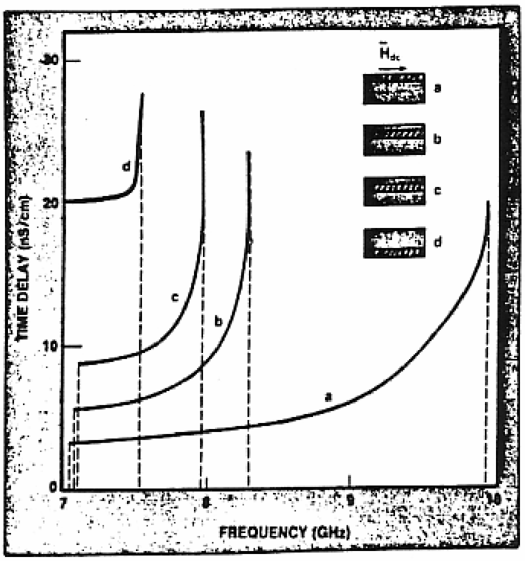

Fig. 3 Time delay vs frequency for various slab positions.

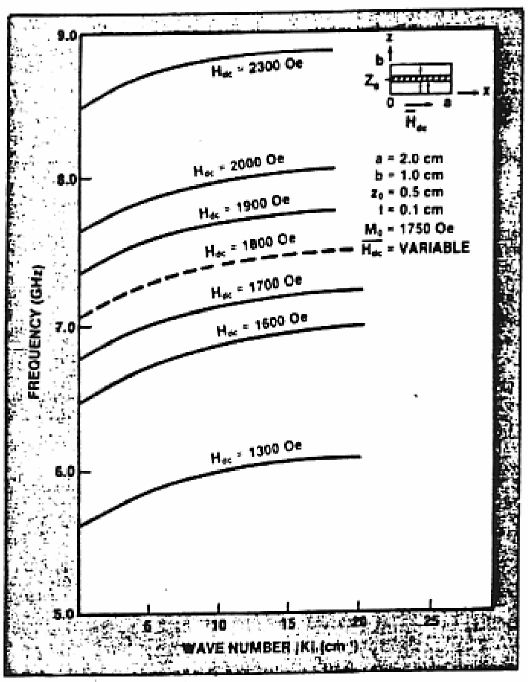

Fig. 4 Effect of magnetic bias field on the dispersion characteristics.

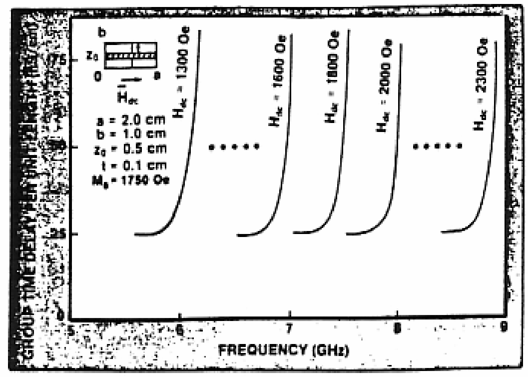

Fig. 5 Effect of magnetic bias field on the group time delay characteristics.

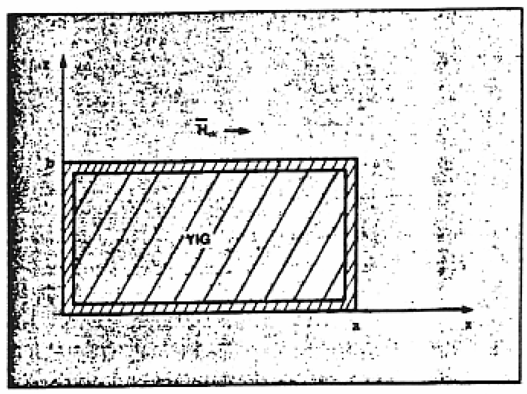

Fig. 6 Cross-section of completely filled waveguide.

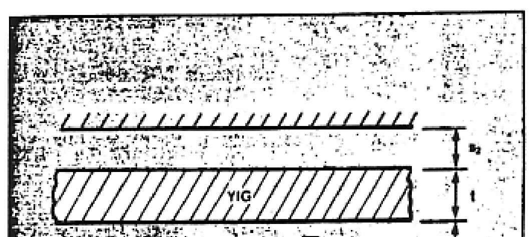

Fig. 7 YIG slab between two ground planes.

$$\begin{bmatrix} \gamma_n' \sinh \gamma_n'(b - z_2) & -K_1K \cosh \gamma_n z_2 + \mu\gamma_n \cosh \gamma_n z_2 & -K_1K \sinh \gamma_n z_2 + \mu\gamma_n \cosh \gamma_n z_2 & 0 \\ \cosh \gamma_n'(b - z_2) & -\cosh \gamma_n z_2 & -\sinh \gamma_n z_2 & 0 \\ 0 & \cosh \gamma_n z_1 & \sinh \gamma_n z_1 & -\cosh \gamma_n' z_1 \\ 0 & -K_1K \cosh \gamma_n z_1 + \mu\gamma_n \sinh \gamma_n z_1 & -K_1K \sinh \gamma_n z_1 + \mu\gamma_n \cosh \gamma_n z_1 & -\gamma_n' \sinh \gamma_n' z_1 \end{bmatrix} \begin{bmatrix} A_n \\ B_n \\ C_n \\ D_n \end{bmatrix} = 0. \quad (10)$$

From Equation 10, the existence of non-trivial solutions for A_n, B_n, C_n and D_n requires the determinant of the coefficient matrix to be set to zero. This yields the following dispersion relation:

$$-\tanh \gamma_n t[K_1^2K^2 - \mu^2\gamma_n^2 - \gamma_n'^2 \tanh \gamma_n' s_2 \tanh \gamma_n' s_1 - K_1 K\gamma_n'(\tanh \gamma_n' s_2 - \tanh \gamma_n' s_1)] + \mu\gamma_n\gamma_n'(\tanh \gamma_n' s_2 + \tanh \gamma_n' s_1) = 0, \quad (11)$$

where t is the thickness of the slab and s_1 and s_2 are thicknesses of the air regions III and I.

An alternate form of Equation 11 is given by

$$e^{2\gamma_n t} = \frac{(\mu\gamma_n - K_1K - \gamma_n' \tanh \gamma_n' s_2)(\mu\gamma_n + K_1K - \gamma_n' \tanh \gamma_n' s_1)}{(\mu\gamma_n + K_1K + \gamma_n' \tanh \gamma_n' s_2)(\mu\gamma_n - K_1K + \gamma_n' \tanh \gamma_n' s_1)}. \quad (12)$$

Numerical Results

A computer program was developed to provide numerical solutions of Equation 11. The computed results for the first node (n = 1) are presented in Figure 2. In this figure the dispersion relations for a 2.0 x 1.0 cm waveguide with a YIG film of thickness t = 0.1 cm are presented for various positions of the YIG slab. The dispersion curves change greatly with the film position. In these computations, the values of DC magnetic field and saturation magnetization are assumed to be H_0 = 1800 Oe and M_0 = 1750 Oe, respectively.

Another important feature is the time delay per unit length (τ_d) given by the relation $\tau_d = (\partial\omega/\partial k)^{-1}$. In Figure 3, the time delay for different slab positions is shown.

The effect of magnetic field on the dispersion characteristics is presented in Figures 4 and 5. Increasing the value of the DC magnetic field would simply shift the dispersion curves upward as depicted in Figure 4. The corresponding group time delay per unit length would accordingly shift, as shown in Figure 5.

Degenerate Cases

Several degenerate cases of this formulation reduce to problems that have been investigated previously. Three of these cases are stated below.

1. Filled Guide

The case corresponds to $s_1 = 0$ and $s_2 = 0$ and is shown in Figure 6. From Equation 11 the following expression is obtained:

$$(\tanh \gamma_n b)\, K_1^2 K^2 - \mu^2\gamma_n{}^2) = 0. \quad (13)$$

Setting the term in the first parentheses to zero in Equation 13 gives

$$\tanh (\gamma_n b) = 0. \quad (14)$$

If $\mu < 0$, the solution to Equation 14 is given by:

$$\gamma_n = j\, \frac{m_\pi}{b}, \; m = 1, 2, 3 \ldots. \quad (15)$$

Combining Equation 15 with Equation 9 yields

$$K^2 = \frac{-1}{\mu}\left(\frac{n\pi}{a}\right)^2 - \left(\frac{m\pi}{b}\right)^2, \; \mu < 0. \quad (16)$$

Equation 16 provides the dispersion relations for magnetostatic volume wave (MSVW). For $\mu > 0$, setting the terms in the second parenthesis to zero gives:

$$\gamma^2 n = K_1^2 K^2/\mu^2. \quad (17)$$

Combining Equation 17 with Equation 9 yields

$$K^2 = \frac{(n\pi/a)^2}{(K_1^2/\mu - \mu)}, \; \mu > 0. \quad (18)$$

Equation 18 gives the dispersion relations for magnetostatic surface wave (MSSW). These are the same results reported by Auld and Mehta.[3]

2. Infinite-Width YIG Between Ground Planes

If $a \to \infty$, the problem reduces to that of Figure 7. From Equation 12 the following relation is obtained:

$$e^{2Kt} = \frac{(\mu - K_1 - \tanh Ks_1)(\mu + K_1 - \tanh Ks_2)}{(\mu + K_1 + \tanh Ks_1)(\mu - K_1 + \tanh Ks_2)}.$$

These are the same results as those reported by Weinberg.[13]

3. Infinite Slab in Free Space

Letting $a \to \infty$, $s_1 \to \infty$ and $s_2 \to \infty$ yields

$$e^{2Kt} = \frac{(\omega_M/2)^2}{\left(\omega_0 + \frac{\omega_M}{2}\right)^2 - \omega^2}.$$

These are the same results reported by Adam et al.[5]

Conclusion

The propagation and time delay characteristics of magnetostatic waves in a waveguide partially filled with a YIG slab were studied. Numerical results were presented for several chosen configurations over a frequency range of 7.0 to 10.0 GHz. The dependence of the dispersion relation and time delay per unit length on the external magnetic bias field and position of the YIG slab were presented. The conclusion is that the position of the YIG slab greatly affects the dispersion curves. Moreover, with a variable external magnetic bias field, the device can be tuned to operate in any desired frequency range.

Finally, the analysis and the computed results presented in this paper not only pave the way for the analysis of a more important general case (i.e., when $x_0 \neq 0$), but also serve as a good means of checking the accuracy of any numerical results obtained for the general case. ■

References

1. Stiglitz, M.R., J.C. Sethares, "Magnetostatic Waves Take Over Where SAWs Leave Off," *Microwave Journal*, Vol. 25, No. 2, pp. 18-111, Feb. 1982.

[Continued on page 140]

2. Owens, J.M., R.L. Carter, C.V. Smith, Jr., "Magnetostatic Waves, Microwave SAW?" 1980 IEEE Ultrasonic Symp. Proc., Boston, MA, pp. 506-512, Nov. 1980.
3. Collins, J.H., J.M. Owens, C.V. Smith, Jr., "Magnetostatic Wave Signal Processing," 1977 Ultrasonic Symp. Proc., Phoenix, AZ, pp. 541-552, Oct. 1977.
4. Morgenthaler, F.R., "MW Signal Processing with Magnetostatic Waves and Modes," *Microwave Journal*, Vol. 25, No. 2, pp. 83-90, Feb. 1982.
5. Adam, J.D., M.R. Daniel, T.W. O'Keefe, "Magnetostatic Wave Devices," *Microwave Journal*, Vol. 25, No. 2, pp. 95-99, Feb. 1982.
6. Vittoria, C., N.D. Wilsey, "Magnetostatic Wave Propagation Losses in an Anisotropic Insulator," *Journal Appl. Phys.*, Vol. 45, No. 1, pp. 414-420, Jan. 1974.
7. Sethares, J.C., M.R. Stiglitz, "Propagation Loss and MSSW Delay Lines," *IEEE Trans. on Magnetics*, Vol. MAG-10, No. 3, pp. 787-790, Sept. 1974.
8. Vittoria, C., D. Webb, P. Lubitz, H. Lessoff, "Magnetostatic Propagation Loss in Thin Films of Liquid Phase Epitaxy YIG," IEEE Trans. on Magnetics, Vol. MAG-11, No. 5, pp. 1259-1261, Sept. 1975.
9. Adam, J.D., J.H. Collins, J.M. Owens, "Microwave Device Applications of Epitaxial Magnetic Garnets," *The Radio and Electronic Engineer*, Vol. 45, No. 12, pp. 738-748, Dec. 1975.
10. Adam, J.D., R.W. Patterson, T.W. O'Keefe, "Magnetostatic Wave Transducers," *Journal Appl. Phys.*, Vol. 49, No. 3, Part 2, pp. 1797-1799, March 1978.
11. Damon, R.W., J.R. Eshbach, "Magnetostatic Modes of a Ferrimagnetic Slab," *Journal Phys. Chem. Solids*, Vol. 19, No. 3/4, pp. 308-320, May 1961.
12. Tsai, M.C., H.J. Wu, J.M. Owens, C.V. Smith, Jr., "Magnetostatic Propagation for Uniform Normally Magnetized Multilayer Planar Structure," AIP Conf. Proc., Pittsburgh, PA, No. 34, pp. 280-282, June 1976.
13. Weinberg, I.J., "Dispersion Relations for Magnetostatic Waves," 1980 IEEE Ultrasonic Symp. Proc., Boston, MA, pp. 557-561, Nov. 1980.
14. Daniel, M.R., J.D. Adam, T.W. O'Keefe, "Linearly Dispersive Delay Lines at Microwave Frequencies Using Magnetostatic Waves," 1979 IEEE Ultrasonics Symp. Proc., New Orleans, LA, pp. 806-809, Sept. 1979.
15. Young, P., "Effect of Boundary Conditions on the Propagation of Surface Magnetostatic Waves in a Transversely Magnetized Thin YIG Slab," Electronics Letters, Vol. 5, No. 18, pp. 429-431, Sept. 1969.
16. Auld, B.A., K.B. Mehta, "Magnetostatic Waves in a Transversely Magnetized Rectangular Rod," *Journal Appl. Phys.*, Vol. 38, No. 10, pp. 4081-4082, Sept. 1967.
17. Lax, B., K.J. Button, *Microwave Ferrites and Ferrimagnetics*, McGraw-Hill Book Co., Inc., New York, pp. 145-151, 1962.
18. Lax, B., K.J. Button, ibid., McGraw-Hill Book Co., Inc., New York, pp. 157-164, 1962.

Massoude Radmanesh *received his undergraduate degree in electrical engineering in 1978 from Pahlavi University, Shiraz, Iran. He earned his MSEE and PhD degrees in electrical engineering and microwave electronics at the University of Michigan, Ann Arbor, MI in 1980 and 1984, respectively. During his studies at the University of Michigan, he was working on microwave solid-state devices, in particular, MSW devices and FET modeling with Professor G.I. Haddad.*

Since 1984 he has been a faculty member at the Electrical and Computer Engineering Department at GMI Engineering and Management Institute, Flint, MI.

He has written several papers on magnetostatic wave propagation in a YIG-loaded waveguide; they are currently in the process of being published. His main areas of interest are microwave solid-state devices, microwave integrated circuits and wave propagation in anisotropic media.

Chiao-min Chu *received his PhD in electrical engineering from the University of Michigan in 1952. Since then he has held several appointments on the research staff at the University of Michigan. He joined the electrical engineering faculty of the University of Michigan as an assistant professor in 1956 and was promoted to full professor in 1983.*

He conducts research in electrical transmission, wave propagation and scattering of waves by conducting and dielectric particles, including scattering from terrain and the sea. He is currently conducting research in the area of wave propagation through anisotropic and random media and the statistical analysis of signals scattered from random surfaces.

George I. Haddad *(S-57, M'61, SM'66, F'72) was born in Aindara, Lebanon on April 7, 1935. He received the BSE, MSE, and PhD degrees in electrical engineering in 1956, 1958, and 1963, respectively from the University of Michigan, Ann Arbor.*

From 1957 to 1958 he was associated with the Engineering Research Institute of The University of Michigan, where he was engaged in research on electromagnetic accelerators. In 1958 he joined the Electron Physics Laboratory, where he was engaged in research on masers, parametric amplifiers, detectors and electron-beam devices.

He is presently associated with the Solid-State Electronics Laboratory and doing research in microwave and mm-wave solid-state devices and monolithic integrated circuits. He served as director of the Electron Physics Laboratory from 1968 to 1975. From 1960 to 1969 he served successively as instructor, assistant professor and associate professor in the Electrical Engineering Department. He is presently a professor and chairman of the Department of Electrical Engineering and Computer Science.

Haddad received the 1970 Curtis W. McGraw Research Award of the American Society for Engineering Education for outstanding achievements by an engineering teacher; he received the College of Engineering Excellence in Research Award in 1985. He is a member of Eta Kappa Nu, Sigma Xi, Phi Kappa Phi, Tau Beta Pi and the American Society for Engineering Education.